

Relativistic coupled-cluster theory of nuclear spin-dependent parity non-conservation

B. K. Mani* and D. Angom†

Physical Research Laboratory, Navarangpura-380009, Gujarat, India

We have developed a relativistic coupled-cluster theory to incorporate nuclear spin-dependent interaction Hamiltonians perturbatively. In this theory, the coupled-cluster operators in the electronic sector are defined as tensor operators of rank one and we introduce suitable diagrammatic representations. For properties calculations, the electronic part is first calculated and later coupled to the nuclear spin part. The method is ideal to calculate parity violating nuclear spin-dependent electric dipole transition amplitudes, $E1_{\text{PNC}}^{\text{NSD}}$, of heavy atoms. To validate the proposed method the $E1_{\text{PNC}}^{\text{NSD}}$ of the transition $6\ ^2S_{1/2} \rightarrow 7\ ^2S_{1/2}$ in ^{133}Cs is calculated for selected MBPT diagrams and compared with the results from our theory.

PACS numbers: 31.15.bw, 32.10.Fn, 31.15.vj, 31.15.am

I. INTRODUCTION

Experimental observation of nuclear spin dependent (NSD) parity non-conservation (PNC) is a signature of nuclear anapole moment (NAM) [1]. It is the most dominant NSD-PNC effect among three possible sources. The other two are: combination of hyperfine and nuclear spin-independent PNC; and spin-dependent Z exchange between electrons and nucleus. To date, the most precise atomic PNC measurement, of atomic Cs, has provided the only experimental evidence of NAM [2]. One major hurdle to a clear observation of nuclear anapole moment is the large nuclear spin-independent (NSI) signal, which overwhelms the NSD signature. However, proposed experiments with single Ba^+ ion [3] could probe PNC in the $s_{1/2} - d_{5/2}$ transition, where the NSI component is zero. This could then provide an unambiguous observation of NSD-PNC and NAM in particular. The ongoing experiments with atomic Ytterbium [4] is another possibility, the $6s^2\ ^1S_0 - 6s5d\ ^3D_2$ transition, to observe NSD-PNC with minimal mixture from the NSI component. One crucial input, which is also the source of large uncertainty, to extract the value of NAM and nuclear weak charge in NSI-PNC is the input from atomic theory calculations. In the case of isotope chain measurements, like in Yb, the PNC observable is a ratio. Atomic theory contributions then cancel and parameters can be extracted without atomic theory calculations. However, results from atomic theory calculations are important in estimating the expected value of PNC transition amplitudes and extracting NAM does require results from atomic theory. For these reasons, it is important to employ reliable and accurate many-body theory in the atomic theory calculations.

Recently, atomic theory calculations have investigated the NSD-PNC of Ba^+ and Ra^+ using the atomic many-body perturbation theory (MBPT) [5]. Another recent work reports the theoretical estimate of the NSD-PNC

observable of Yb [6] and the calculations are based on the CI-MBPT method [7]. There is also an earlier work on NSD-PNC of Yb using the same method [8]. Very recently, the CI-MBPT method is used to calculate the NSD-PNC observables of Ba^+ , Yb^+ and Ra^+ [9]. Besides the methods mentioned, earlier works on Ba^+ [10] and Yb [11] used configuration interaction (CI). To date, coupled-cluster theory (CCT) considered as one of the most reliable and accurate many-body theory has not been used in the NSD-PNC calculations. The difficulty of developing a suitable theory stems from the complications of dealing with the nuclear spin dependent interaction. In a previous paper of ours we reported the development of a relativistic coupled-cluster (RCC) theory to incorporate nuclear spin-dependent interaction in a consistent scheme [12]. In this work we provide elaborate details of the theory and touch upon related subtle issues.

The coupled-cluster (CC) theory [13, 14] is one of the most reliable many-body theory to incorporate electron correlation in atomic calculations. In atomic physics, the relativistic coupled-cluster (RCC) theory has been used extensively in atomic properties calculations, for example, hyperfine structure constants [15, 16], electric dipole moments [17, 18], and electromagnetic transition properties [19, 20]. In atomic PNC calculations too, RCC is the preferred theory and several groups have used it to calculate NSI-PNC of atoms [21–23]. However, the calculations in Ref. [21] are entirely based on RCC with a variation we refer to as perturbed RCC (PRCC), where as the calculations in Ref. [22, 23] are based on sum over states with CC wave functions. Naturally, the former incorporates electron correlation more precisely than the later approach.

In this work we provide a detailed explanation on the approach we have adopted to incorporate nuclear spin-dependent interaction Hamiltonian as a perturbation in RCC theory. In Section. II, we give a very short account of RCC theory to serve as a quick reference. We then give the details of our formulation to represent a NSD interaction perturbed CC operator in Section. III. PRCC equations of closed-shell and one-valence systems is derived in this section. To simplify angular factor cal-

* bkmani@prl.res.in

† angom@prl.res.in

culations, the calculations in the electronic sector is separated out. Based on this the calculation of NSD-PNC observable, in the electronic sector, is described in Section. IV. Next section, Section. V, describes the coupling of results from the electronic sector with the nuclear spin. This completes the theoretical development and then, the correctness of theory is verified in Section. VI. For which, we use MBPT results and calculate the NSD-PNC of the $6\ ^2S_{1/2} \rightarrow 7\ ^2S_{1/2}$ transition in Cs. We then conclude and the angular factors of all the diagrams in the linearized PRCC are given in the Appendix.

II. BRIEF REVIEW OF RCC

For N -electron atoms or ions the Dirac-Coulomb Hamiltonian, appropriate to account for relativistic effects, is

$$H^{\text{DC}} = \sum_{i=1}^N [c\boldsymbol{\alpha}_i \cdot \mathbf{p}_i + (\beta_i - 1)c^2 - V_N(r_i)] + \sum_{i<j} \frac{1}{r_{ij}}, \quad (1)$$

where $\boldsymbol{\alpha}_i$ and β are the Dirac matrices, \mathbf{p} is the linear momentum, $V_N(r)$ is the nuclear Coulomb potential and last term is the electron-electron Coulomb interactions. For one-valence systems it satisfies the eigen value equation

$$H^{\text{DC}}|\Psi_v\rangle = E_v|\Psi_v\rangle, \quad (2)$$

where $|\Psi_v\rangle$ and E_v are the atomic state and energy respectively. In the CC method, the atomic state is expressed in terms of T and S , the closed-shell and one-valence cluster operators respectively, as

$$|\Psi_v\rangle = e^{T^{(0)}} [1 + S^{(0)}] |\Phi_v\rangle, \quad (3)$$

where $|\Phi_v\rangle$ is the one-valence Dirac-Fock reference state. It is obtained by adding an electron to the closed-shell reference state, $|\Phi_v\rangle = a_v^\dagger|\Phi_0\rangle$. In the coupled-cluster singles doubles (CCSD) approximation $T^{(0)} = T_1^{(0)} + T_2^{(0)}$ and are the solutions of the nonlinear coupled equations

$$\langle \Phi_a^p | \bar{H}_N | \Phi_0 \rangle = 0, \quad (4a)$$

$$\langle \Phi_{ab}^{pq} | \bar{H}_N | \Phi_0 \rangle = 0, \quad (4b)$$

where $\bar{H}_N = e^{-T^{(0)}} H_N e^{T^{(0)}}$ is the similarity transformed Hamiltonian and the normal order Hamiltonian $H_N = H - \langle \Phi_0 | H | \Phi_0 \rangle$. The states $|\Phi_a^p\rangle$ and $|\Phi_{ab}^{pq}\rangle$ are the singly and doubly excited determinants, respectively and $abc\dots(pqr\dots)$ denote occupied (virtual) orbitals. The details of the derivation are given in Ref. [24]. Like in $T^{(0)}$, the one-valence cluster operator $S^{(0)}$ in the CCSD approximation is $S^{(0)} = S_1^{(0)} + S_2^{(0)}$. And these are the solutions of

$$\langle \Phi_a^p | \bar{H}_N + \{\bar{H}_N S^{(0)}\} | \Phi_v \rangle = E_v^{\text{att}} \langle \Phi_a^p | S_1^{(0)} | \Phi_v \rangle, \quad (5a)$$

$$\langle \Phi_{va}^{pq} | \bar{H}_N + \{\bar{H}_N S^{(0)}\} | \Phi_v \rangle = E_v^{\text{att}} \langle \Phi_{va}^{pq} | S_2^{(0)} | \Phi_v \rangle, \quad (5b)$$

where $E_v^{\text{att}} = E_v - E_0$, is the attachment energy of the valence electron. In our previous work [25], we provide details of the derivation.

III. PERTURBED CC WAVE FUNCTION

Time independent perturbation theory is the standard procedure to incorporate external perturbations or additional interactions in atomic many-body calculations. However, a basic requirement of perturbative calculations is a complete set of intermediate atomic states, which is non-trivial to generate. The perturbed CC method [24, 26, 27], on the other hand, implicitly accounts for all the possible intermediate states. In this work, we consider the perturbation as the nuclear spin-dependent parity non-conserving (PNC) interaction

$$H_{\text{PNC}}^{\text{NSD}} = \frac{G_F \mu'_W}{\sqrt{2}} \sum_i \boldsymbol{\alpha}_i \cdot \mathbf{I} \rho_N(r), \quad (6)$$

where μ'_W is the weak nuclear moment of the nucleus and $\rho_N(r)$ is the nuclear density. The weak nuclear moment is expressed in terms of the neutron and proton numbers $\mu'_W = 2(ZC_{1p} + NC_{1n})$, where C_{1p} and C_{1n} are respectively the vector electron and the axial vector nucleon coupling coefficients. There are two complications arising from the nuclear spin operator I in $H_{\text{PNC}}^{\text{NSD}}$. First, the cluster operators in the electron space are rank one operators, and second, the atomic states in the one-valence sector are eigenstates of total angular momentum $\mathbf{F} = \mathbf{I} + \mathbf{J}$. Both of these are relatively simple to incorporate at lower order MBPT calculations, however, implementing these in non-perturbative theory like RCC is nontrivial. Accordingly, the method we have developed and implemented in the current work are very different from our previous works [24, 27]. The other simplifying feature of the previous works is, the methods developed were for closed-shell systems where the total electronic angular momentum $\mathbf{J} = 0$.

With the PNC interaction, the total atomic Hamiltonian is

$$H_A = H^{\text{DC}} + \lambda H_{\text{PNC}}^{\text{NSD}}, \quad (7)$$

where λ is the perturbation parameter. As $H_{\text{PNC}}^{\text{NSD}}$ mixes atomic states of opposite parities, the eigenvalue equation is modified to

$$H_A |\tilde{\Psi}_v\rangle = E_v |\tilde{\Psi}_v\rangle. \quad (8)$$

Note that the first order energy correction $E^1 = \langle \Psi_0 | H_{\text{PNC}}^{\text{NSD}} | \Psi_0 \rangle = 0$ as $H_{\text{PNC}}^{\text{NSD}}$ is an odd parity interaction Hamiltonian. This is taken into account while writing the above eigenvalue equation. Here $|\tilde{\Psi}_v\rangle$ are the mixed parity atomic states and to first order in perturbation

$$|\tilde{\Psi}_v\rangle = |\Psi_v\rangle + \sum_I |\Psi_I\rangle \frac{\langle \Psi_I | H_{\text{PNC}}^{\text{NSD}} | \Psi_v \rangle}{E_v - E_I}. \quad (9)$$

If $|\Psi_v\rangle$ and $|\bar{\Psi}_v\rangle$ are atomic states of same parity, then the $H_{\text{PNC}}^{\text{NSD}}$ induced electric dipole ($E1$) transition amplitude is

$$E1_{\text{PNC}}^{\text{NSD}} = \langle \tilde{\Psi}_w \| \mathbf{D} \| \tilde{\Psi}_v \rangle, \quad (10)$$

where \mathbf{D} is the dipole operator. The perturbation expression in Eq. (9) require a complete set of intermediate atomic states $|\Psi_I\rangle$. This, as mentioned at the beginning of the section, is non-trivial to obtain in atomic many-body calculations. Summation over intermediate states is circumvented when $E1_{\text{PNC}}^{\text{NSD}}$ is calculated with CC atomic states. For this define a new set of cluster operators $\mathbf{T}^{(1)}$, which unlike $T^{(0)}$ connects the reference state to opposite parity states. This is the result of incorporating one order of $H_{\text{PNC}}^{\text{NSD}}$ and for this reason we refer to $\mathbf{T}^{(1)}$ as the perturbed cluster operators. Although hyperfine states are natural to $H_{\text{PNC}}^{\text{NSD}}$, cluster operator $\mathbf{T}^{(1)}$ is defined to operate only in the electronic space and is a rank one operator. So, the mixed parity atomic state in RCC is

$$|\tilde{\Psi}_0\rangle = e^{T^{(0)} + \lambda \mathbf{T}^{(1)} \cdot \mathbf{I}} |\Phi_0\rangle. \quad (11)$$

The scalar product with the nuclear spin \mathbf{I} in the exponent restores $\mathbf{T}^{(1)}$ to the correct form of the wave operator. At this point it is convenient to separate out the electronic part of the interaction Hamiltonian

$$\mathbf{H}_{\text{elec}}^{\text{NSD}} = \frac{G_{\text{F}} \mu'_{\text{W}}}{\sqrt{2}} \sum_i \tilde{\alpha}_i \rho_{\text{N}}(r), \quad (12)$$

which operates only in the electronic space, so that

$$H_{\text{PNC}}^{\text{NSD}} = \mathbf{H}_{\text{elec}}^{\text{NSD}} \cdot \mathbf{I}. \quad (13)$$

The remaining part of this section describe how to arrive at a consistent representation of $\mathbf{T}^{(1)}$ and extension of the method to one-valence systems, where $\mathbf{S}^{(1)}$ are the perturbed cluster operators.

A. MBPT wavefunctions

To define the multipole and parity selection rules of $T^{(1)}$, we examine the second order MBPT wave function with $H_{\text{PNC}}^{\text{NSD}}$ as one of the perturbations. From the generalized Bloch equation [28], the total wave operator is [5]

$$\Omega_v = \sum_{n=1}^{\infty} \Omega_{v,0}^{(n)} + \sum_{n=1}^{\infty} \Omega_{v,1}^{(n)}. \quad (14)$$

Here $\Omega_{v,0}^{(n)}$ has n orders of residual Coulomb interaction, where as $\Omega_{v,1}^{(n)}$ has one order of $H_{\text{PNC}}^{\text{NSD}}$ and n orders of residual Coulomb interaction. Following which the mixed parity state

$$|\tilde{\Psi}_v\rangle = |\Psi_v\rangle + |\bar{\Psi}_v\rangle = \sum_{n=1}^{\infty} \Omega_{v,0}^{(n)} |\Phi_v\rangle + \sum_{n=1}^{\infty} \Omega_{v,1}^{(n)} |\Phi_v\rangle, \quad (15)$$

where $|\bar{\Psi}_v\rangle$ is the opposite parity component arising from the $H_{\text{PNC}}^{\text{NSD}}$. The first order wave function is then,

$$|\tilde{\Psi}_v^1\rangle = |\Psi_v^1\rangle + |\bar{\Psi}_v^1\rangle = \left[1 + \Omega_{v,0}^{(1)}\right] |\Phi_v\rangle + \Omega_{v,1}^{(1)} |\Phi_v\rangle. \quad (16)$$

Although, notation wise $\Omega_{v,1}^{(1)}$ seem first order, it is second order in perturbation: one order each in residual Coulomb interaction and $H_{\text{PNC}}^{\text{NSD}}$. For model space consisting of same parity states

$$\left[\Omega_{v,1}^{(1)}, H_0\right] P = Q H_{\text{PNC}}^{\text{NSD}} \Omega_{v,0} P + Q V_{\text{res}} \Omega_{v,1}^{(0)} P. \quad (17)$$

Here, and P and Q are the projection operators of the model and complementary spaces, respectively, H_0 is the Dirac-Fock Hamiltonian, V_{res} is the residual Coulomb interaction and the zeroth order mixed parity wave operator

$$\Omega_{v,1}^{(0)} P = Q \frac{1}{E_v^0 - H_0} Q H_{\text{PNC}}^{\text{NSD}} P. \quad (18)$$

Using $\Omega_{v,1}^{(0)}$ and $\Omega_{v,0}^{(1)}$, we may compute $E1_{\text{PNC}}$ to third order in perturbation, the details of which are discussed in Ref. [5].

B. Perturbed cluster operator representation

The expression of $\Omega_{v,1}^{(1)}$ and associated selection rules are what we need to arrive at a consistent description of $T^{(1)}$. In Fig. 1(a) we show an MBPT wave function

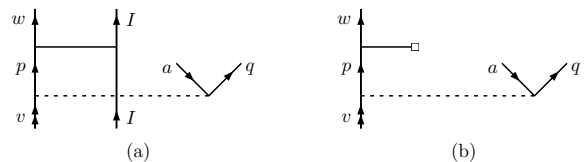


FIG. 1. Second order MBPT diagram where interaction Hamiltonian $H_{\text{PNC}}^{\text{NSD}}$ operates on the particle state p . (a) Diagrammatic representation of $H_{\text{PNC}}^{\text{NSD}}$ in the electronic and nuclear spin space. (b) Diagrammatic representation within the electronic space only where the PNC interaction Hamiltonian is $H_{\text{elec}}^{\text{NSD}}$. Line terminated with square represents the PNC interaction.

diagram of $\Omega_{v,1}^{(1)}$ arising from the second term in Eq. (18). The algebraic expression of the diagram is

$$\frac{G_{\text{F}} \mu'_{\text{W}}}{\sqrt{2}} \sum_p |wqI\rangle \frac{\langle wI | \boldsymbol{\alpha} \cdot \mathbf{I} \rho_{\text{N}}(r) | pI \rangle \langle pqI | V_{\text{res}} | vaI \rangle}{(\epsilon_w - \epsilon_p)(\epsilon_v + \epsilon_a - \epsilon_p - \epsilon_q)}, \quad (19)$$

where ϵ_i are the orbital energies. The states $|\dots I\rangle$ represent uncoupled atomic states comprising of electronic and nuclear states.

On closer examination, the component of $H_{\text{PNC}}^{\text{NSD}}$ which operates in the nuclear subspace is diagonal. So, for further calculations, we separate out the matrix elements

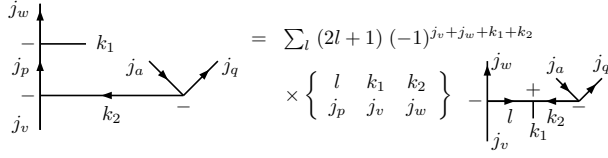


FIG. 2. Angular reduction of the second order MBPT diagram. The remnant angular momentum diagram on the right is representative of the multipole structure of PRCC double excitation cluster operators $T_2^{(1)}$ and $S_2^{(1)}$.

in the electronic subspace and combine with the nuclear part at the end of the calculations. For the MBPT diagram considered earlier Fig. 1(a), the electronic part is as shown in Fig. 1(b). The corresponding algebraic expression is

$$\frac{G_F \mu'_W}{\sqrt{2}} \sum_p \frac{\langle w | \alpha \rho_N(r) | p \rangle \langle p q | V | v a \rangle}{(\epsilon_w - \epsilon_p)(\epsilon_v + \epsilon_a - \epsilon_p - \epsilon_q)}. \quad (20)$$

Details of the angular reduction when electronic state is coupled with the nuclear state are discussed in the later sections of the paper. Like wise, the perturbed cluster operators $\mathbf{T}^{(1)}$, as defined earlier operate only in the electronic. For this consider the angular part of the matrix elements in Eq. (20), the diagrammatic representation is shown in Fig. 2. The angular diagrams are based on the conventions used in Lindgren and Morrison [28] and the same is followed in the remaining of the paper while referring to angular momentum diagrams. In the figure, the angular diagram on the right hand side indicates the multipole structure of the $T_2^{(1)}$ and like the electron-electron Coulomb interaction

$$\mathbf{T}_2^{(1)} = \sum_{abpq} \sum_{l, k_2} \tau_{ab}^{pq}(l, k_2) \{ \mathbf{C}_l(\hat{r}_1) \mathbf{C}_{k_2}(\hat{r}_2) \}^1, \quad (21)$$

where \mathbf{C}_i are c-tensor operators and $\{\dots\}^1$ indicates the two c-tensor operators couple to a rank one tensor operator. Following general rules of coupling tensor operators, the rank of the tensor operators must satisfy the triangular conditions $|j_w - j_v| \leq l \leq (j_w + j_v)$, $|j_a - j_q| \leq k_2 \leq (j_a + j_q)$ and $|l - k_2| \leq 1 \leq (l + k_2)$. Effectively, $\mathbf{T}^{(1)}$ is a rank one operator in the electronic subspace and forms a scalar operator after coupling with \mathbf{I} . The other important difference from the $T^{(0)}$ is the parity selection rule at the vertices. The combined parities at the vertices are opposite $(-1)^{l_w+l_v} = -(-1)^{l_a+l_q}$. After a similar analysis, the singles operator is

$$\mathbf{T}_1^{(1)} = \sum_{ap} \tau_a^p \mathbf{C}_1(\hat{r}). \quad (22)$$

Based on the multipole structures, the perturbed cluster operators are diagrammatically represented as shown in Fig. 3. For the doubles $\mathbf{T}_2^{(1)}$, to indicate the multipole structure, an additional line is added to the interaction line.

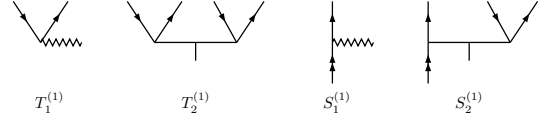


FIG. 3. Diagrammatic representation of the single and double excitation perturbed cluster operators in closed shell and one- valence sectors. The extra line in the $T_2^{(1)}$ and $S_2^{(1)}$ is to indicate the multipole structure of the operators.

C. Closed-shell systems

The mixed parity states, eigenstates of H_A , in the perturbed relativistic coupled-cluster (PRCC) is as given in Eq. (11). However, as $H_{\text{PNC}}^{\text{NSD}}$ is considered to first order only, it is sufficient to consider up to linear terms in the expansion of $e^{\lambda \mathbf{T}^{(1)} \cdot \mathbf{I}}$. The PRCC atomic state is then

$$|\tilde{\Psi}_0\rangle = e^{T^{(0)}} [1 + \lambda \mathbf{T}^{(1)} \cdot \mathbf{I}] |\Phi_0\rangle. \quad (23)$$

The cluster operator $\mathbf{T}^{(1)}$, as described earlier, incorporates $\mathbf{H}_{\text{elec}}^{\text{NSD}}$ to first order and residual Coulomb interaction to all order. The closed-shell equivalent of Eq. (8), the mixed parity eigenvalue equation, is

$$(H^{\text{DC}} + \lambda \mathbf{H}_{\text{elec}}^{\text{NSD}} \cdot \mathbf{I}) |\tilde{\Psi}_0\rangle = E_0 |\tilde{\Psi}_0\rangle. \quad (24)$$

From the definition of the coupled-cluster mixed parity state in Eq. (23), the eigen value equation in terms of the coupled-cluster wavefunction is

$$(H^{\text{DC}} + \lambda \mathbf{H}_{\text{elec}}^{\text{NSD}} \cdot \mathbf{I}) e^{T^{(0)}} [1 + \lambda \mathbf{T}^{(1)} \cdot \mathbf{I}] |\Phi_0\rangle = E_0 e^{T^{(0)}} [1 + \lambda \mathbf{T}^{(1)} \cdot \mathbf{I}] |\Phi_0\rangle. \quad (25)$$

In terms of H_N , defined earlier, the eigenvalue equation is simplified to

$$(H_N + \lambda \mathbf{H}_{\text{elec}}^{\text{NSD}}) e^{T^{(0)}} [1 + \lambda \mathbf{T}^{(1)} \cdot \mathbf{I}] |\Phi_0\rangle = \Delta E_0 e^{T^{(0)}} [1 + \lambda \mathbf{T}^{(1)} \cdot \mathbf{I}] |\Phi_0\rangle, \quad (26)$$

where $\Delta E_0 = E_0 - \langle \Phi_0 | H | \Phi_0 \rangle$ is the closed-shell correlation energy. Retaining terms which are first-order in λ , we get

$$[H_N \mathbf{T}^{(1)} \cdot \mathbf{I} + \mathbf{H}_{\text{elec}}^{\text{NSD}} \cdot \mathbf{I}] e^{T^{(0)}} |\Phi_0\rangle = \Delta E_0 \mathbf{T}^{(1)} \cdot \mathbf{I} e^{T^{(0)}} |\Phi_0\rangle. \quad (27)$$

From here on, for simplicity, we drop the nuclear spin operator \mathbf{I} and work only in the electronic space. At a later stage of the calculations the electronic part is coupled with the nuclear spin. Operating with $e^{-T^{(0)}}$ and projecting on singly and doubly excited states $\langle \Phi_a^p |$ and $\langle \Phi_{ab}^{pq} |$, respectively, we get the CC equations for singles and doubles perturbed cluster amplitudes as

$$\langle \Phi_a^p | \{ \overline{\mathbf{H}_N \mathbf{T}^{(1)}} \} | \Phi_0 \rangle = - \langle \Phi_a^p | \overline{\mathbf{H}_{\text{elec}}^{\text{NSD}}} | \Phi_0 \rangle, \quad (28a)$$

$$\langle \Phi_{ab}^{pq} | \{ \overline{\mathbf{H}_N \mathbf{T}^{(1)}} \} | \Phi_0 \rangle = - \langle \Phi_{ab}^{pq} | \overline{\mathbf{H}_{\text{elec}}^{\text{NSD}}} | \Phi_0 \rangle \quad (28b)$$

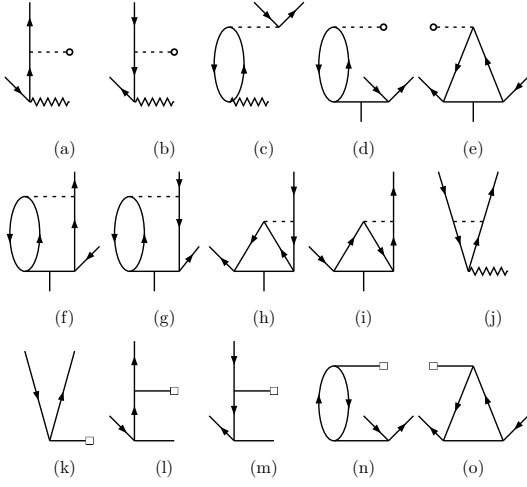


FIG. 4. Diagrams which contribute to the linearized perturbed coupled-cluster equations of the singly excited cluster operator $T_1^{(1)}$.

Where, $\bar{\mathbf{H}}_{\text{elec}}^{\text{NSD}} = e^{-T^{(0)}} \mathbf{H}_{\text{elec}}^{\text{NSD}} e^{T^{(0)}}$, is the similarity transformed PNC interaction Hamiltonian in the electronic subspace. The perturbed cluster operators are solutions of these coupled linear equations. However, the equations are nonlinear in the unperturbed cluster operators $T^{(0)}$. The advantage of separating the cluster operators into two categories $T^{(0)}$ and $\mathbf{T}^{(1)}$ is, the two sets of equations can be solved sequentially. As the $T^{(0)}$ has no dependence on $\mathbf{T}^{(1)}$, the $T^{(0)}$ equations are solved first and then the $\mathbf{T}^{(1)}$ equations are solved. An approximate form of Eq. (28a) and (28b), but which contains all the important many-body effects, are the linearized cluster equations. This is obtained by considering

$$\overline{H_N \mathbf{T}^{(1)}} \approx \overline{H_N \mathbf{T}^{(1)}}, \quad (29a)$$

$$\bar{\mathbf{H}}_{\text{elec}}^{\text{NSD}} \approx \mathbf{H}_{\text{elec}}^{\text{NSD}} + \overline{\mathbf{H}_{\text{elec}}^{\text{NSD}} T^{(0)}}. \quad (29b)$$

The diagrams in the singles and doubles equation arising from $\overline{H_N \mathbf{T}^{(1)}}$ are shown in Fig. 4 and 5, respectively.

The other form of Eq. (29) is to write the equation in terms of specific cluster amplitudes. The singles equation is then,

$$(\epsilon_a - \epsilon_p) \tau_a^p = \mathbf{h}_{pa} + \sum_q \mathbf{h}_{pq} t_a^q - \sum_b \mathbf{h}_{ba} t_b^p + \sum_{bq} \mathbf{h}_{bq} \tilde{t}_{ba}^{qp} + \sum_{bq} \tilde{g}_{b p q a} \tau_b^q + \sum_{bqr} \tilde{g}_{b p q r} \tau_{ba}^{qr} - \sum_{bcq} g_{bcqa} \tilde{\tau}_{bc}^{qp}, \quad (30)$$

where g_{ijkl} and \mathbf{h}_{ij} , are the matrix elements $\langle ij|V|kl\rangle$ and $\langle i|\mathbf{H}_{\text{elec}}^{\text{NSD}}|j\rangle$, respectively, and t_j^i and t_{kl}^{ij} are the unperturbed single and double excitation RCC amplitudes, respectively. For compact notation, we have defined $\tilde{g}_{ijkl} = g_{ijkl} - g_{ijlk}$. Similarly, \tilde{t}_{kl}^{ij} and $\tilde{\tau}_{kl}^{ij}$ are the antisymmetized unperturbed and perturbed CC amplitudes

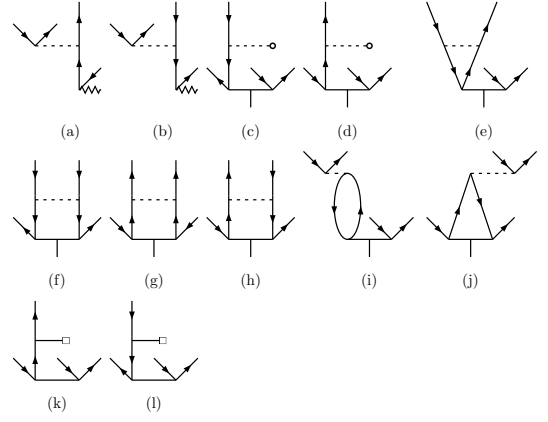


FIG. 5. Diagrams which contribute to the closed-shell linearized perturbed coupled-cluster equations of the doubly excited cluster operator $T_2^{(1)}$.

respectively. The equation of the double excitation perturbed cluster amplitudes is

$$(\epsilon_a + \epsilon_b - \epsilon_p - \epsilon_q) \tau_{ab}^{pq} = \left(\sum_r \mathbf{h}_{pr} t_{ab}^{rq} - \sum_c \mathbf{h}_{ca} t_{cb}^{pq} + \sum_r g_{pqr} \tau_a^r - \sum_c g_{cqa} \tau_c^p + \sum_{rc} g_{pcar} \tilde{\tau}_{cb}^{rq} - \sum_{rc} g_{pcrb} \tau_{ac}^{rq} - \sum_{rc} g_{cpar} \tau_{cb}^{rq} \right) + \left(\begin{matrix} p \leftrightarrow q \\ a \leftrightarrow b \end{matrix} \right) + \sum_{rs} g_{pqrs} \tau_{ab}^{rs} + \sum_{cd} g_{cdab} \tau_{cd}^{pq}. \quad (31)$$

where $\left(\begin{matrix} p \leftrightarrow q \\ a \leftrightarrow b \end{matrix} \right)$ represents terms similar to those within parenthesis but with the combined permutations $p \leftrightarrow q$ and $a \leftrightarrow b$. These equations are similar to the unperturbed cluster equations in Ref. [28]. There is, however, a major difference from the all-order equations of unperturbed cluster operators used in other works [29, 30] which use antisymmetized cluster operators. Here, all order is the same as the linearized coupled-cluster theory and in the antisymmetized representation $t_{ab}^{pq} = -t_{ba}^{pq}$. For our work, which is based on diagrammatic evaluation of angular factors, the representation without antisymmetrization is preferable as it follows directly from the diagrams. To solve Eq. (30) and (31), the expressions of τ_{ab}^{pq} are separated into multipole components and the angular factor of each term in the two equations are given in the Appendix.

D. One-valence systems

From Eq. (24), we may write the perturbed eigenvalue equation of the one-valence system as

$$(H^{\text{DC}} + \lambda \mathbf{H}_{\text{elec}}^{\text{NSD}} \cdot \mathbf{I}) |\tilde{\Psi}_v\rangle = E_v |\tilde{\Psi}_v\rangle. \quad (32)$$

As defined earlier, E_v is the energy of the one-valence system. Similar to the closed-shell case, the perturbed wavefunction in CC theory is

$$|\tilde{\Psi}_v\rangle = e^{T^{(0)}} \left[1 + \lambda \mathbf{T}^{(1)} \cdot \mathbf{I} \right] \left[1 + S^{(0)} + \lambda \mathbf{S}^{(1)} \cdot \mathbf{I} \right] |\Phi_v\rangle, \quad (33)$$

where $\mathbf{S}^{(1)}$ is the perturbed CC operator of the one-valence part. The diagrammatic representation of the valence single and double perturbed cluster operators $\mathbf{S}_1^{(1)}$ and $\mathbf{S}_2^{(1)}$, respectively, are shown in Fig. 3. These are topologically equivalent to the diagrams of the closed-shell operators $\mathbf{T}_1^{(1)}$ and $\mathbf{T}_2^{(1)}$, however, with one of the core lines rotated. The Eq. (33) in terms of the PRCC wavefunction is

$$\begin{aligned} (H + \lambda \mathbf{H}_{\text{elec}}^{\text{NSD}} \cdot \mathbf{I}) e^{T^{(0)}} \left[1 + \lambda \mathbf{T}^{(1)} \cdot \mathbf{I} \right] \left[1 + S^{(0)} \right. \\ \left. + \lambda \mathbf{S}^{(1)} \cdot \mathbf{I} \right] |\Phi_v\rangle = E_v e^{T^{(0)}} \left[1 + \lambda \mathbf{T}^{(1)} \cdot \mathbf{I} \right] \left[1 + S^{(0)} \right. \\ \left. + \lambda \mathbf{S}^{(1)} \cdot \mathbf{I} \right] |\Phi_v\rangle. \end{aligned} \quad (34)$$

To derive the $\mathbf{S}^{(1)}$ equations, like in the closed-shell case, project the above equation on e^{-T} and retain the terms linear in λ . For further simplification, use normal-ordered form of the Hamiltonian, which for the one-valence system is $H_N = H - \langle \Phi_v | H | \Phi_v \rangle$. After these sequence of operations, and retaining only the electronic part like in the closed-shell case, the eigen value equation is modified to

$$\begin{aligned} \left[\bar{H}_N \mathbf{S}^{(1)} + \bar{H}_N \mathbf{T}^{(1)} (1 + S) + \bar{\mathbf{H}}_{\text{elec}}^{\text{NSD}} (1 + S) \right] |\Phi_v\rangle \\ = \left[\Delta E_v \mathbf{S}^{(1)} + \Delta E_v \mathbf{T}^{(1)} (1 + S) \right] |\Phi_v\rangle, \end{aligned} \quad (35)$$

where $\Delta E_v = E_v - \langle \Phi_v | H | \Phi_v \rangle$, is the correlation energy of the one-valence system. Projecting Eq. (35) with the excited determinants $\langle \Phi_v^p |$ and $\langle \Phi_{va}^{pq} |$, we get the perturbed CC equations of the singles and doubles respectively, in the form

$$\begin{aligned} \langle \Phi_v^p | \{ \overline{\bar{H}_N \mathbf{S}^{(1)}} \} + \{ \overline{\bar{H}_N \mathbf{T}^{(1)}} \} + \{ \overline{\bar{H}_N \mathbf{T}^{(1)} S^{(0)}} \} + \bar{\mathbf{H}}_{\text{elec}}^{\text{NSD}} \\ + \{ \overline{\bar{\mathbf{H}}_{\text{elec}}^{\text{NSD}} S^{(0)}} \} | \Phi_v \rangle = \Delta E_v \langle \Phi_v^p | \mathbf{S}_1^{(1)} | \Phi_v \rangle, \end{aligned} \quad (36a)$$

$$\begin{aligned} \langle \Phi_{vb}^{pq} | \{ \overline{\bar{H}_N \mathbf{S}^{(1)}} \} + \{ \overline{\bar{H}_N \mathbf{T}^{(1)}} \} + \{ \overline{\bar{H}_N \mathbf{T}^{(1)} S^{(0)}} \} + \bar{\mathbf{H}}_{\text{elec}}^{\text{NSD}} \\ + \{ \overline{\bar{\mathbf{H}}_{\text{elec}}^{\text{NSD}} S^{(0)}} \} | \Phi_v \rangle = \Delta E_v \langle \Phi_{vb}^{pq} | \mathbf{S}_2^{(1)} | \Phi_v \rangle. \end{aligned} \quad (36b)$$

Where, we have used the relations

$$\langle \Phi_v^p | \mathbf{T}^{(1)} | \Phi_v \rangle = 0, \text{ and } \langle \Phi_v^p | \mathbf{T}^{(1)} S | \Phi_v \rangle = 0, \quad (37)$$

as $\mathbf{T}^{(1)}$, being the cluster operator of closed-shell sector, does not contribute to the CC equation of $\mathbf{S}_1^{(1)}$ and $\mathbf{S}_2^{(1)}$. In terms of specific components, as in Eq. (30), the single

excitation perturbed cluster amplitude equation is

$$\begin{aligned} (\epsilon_v + \Delta E_v - \epsilon_p) \tau_v^p = \mathbf{h}_{pv} + \sum_q \mathbf{h}_{pq} t_v^q - \sum_b \mathbf{h}_{bv} t_b^p \\ + \sum_{bq} \mathbf{h}_{bq} \tilde{t}_{bv}^{qp} + \sum_{bq} \tilde{g}_{bpbv} \tau_b^q + \sum_{bqr} \tilde{g}_{bpbv} \tau_{bv}^{qr} \\ - \sum_{bcq} g_{bcqv} \tilde{t}_{bc}^{qp}. \end{aligned} \quad (38)$$

This is Eq. (30) with two important modifications. First, the valence orbital v replaces the orbital a and second, the single particle energy of v is modified to include the correlation energy. Following similar modifications, the equation of the double excitation cluster amplitudes is

$$\begin{aligned} (\epsilon_v + \Delta E_v + \epsilon_b - \epsilon_p - \epsilon_q) \tau_{vb}^{pq} = \left(\sum_r \mathbf{h}_{pr} t_{vb}^{rq} - \sum_c \mathbf{h}_{cv} t_{cb}^{pq} \right. \\ \left. + \sum_r g_{pqr} \tau_v^r - \sum_c g_{cqv} \tau_c^p + \sum_{rc} g_{pcvr} \tilde{\tau}_{cb}^{rq} \right. \\ \left. - \sum_{rc} g_{pcrb} \tau_{vc}^{rq} - \sum_{rc} g_{cpvr} \tau_{cb}^{rq} \right) + \begin{pmatrix} p \leftrightarrow q \\ v \leftrightarrow b \end{pmatrix} \\ + \sum_{rs} g_{pqr} \tau_{vb}^{rs} + \sum_{cd} g_{cdvb} \tau_{cd}^{pq}. \end{aligned} \quad (39)$$

Angular factors obtained from the closed-shell sector, with replacement of a by v , can be used to rewrite the cluster equations in terms specific multipole components from these equations. With these modifications, the same methods used to solve the $T^{(1)}$ are used to calculate the $S^{(1)}$ cluster amplitudes. The fore going derivations shows that PRCC equations of one-valence sector are not very different from the closed-shell equations. But the same rationale does not apply to two-valence PRCC equations. For two-valence systems, even at the level of RCC, require due considerations on the nature of model space. Properties calculations from the RCC wave functions is another level of sophistication, these and related issues on RCC calculations of two-valence systems is explored in one of our recent works [31].

IV. $E1_{\text{elec}}^{\text{NSD}}$ CALCULATION

In this section, as prelude to the calculation of $E1_{\text{elec}}^{\text{NSD}}$ from the PRCC states, the details of $E1_{\text{PNC}}^{\text{NSD}}$ calculation with MBPT is discussed at the beginning. The MBPT calculation, however, is in the hyperfine states and is equivalent to the PRCC expressions of $E1_{\text{elec}}^{\text{NSD}}$ after coupling with the nuclear states.

A. From MBPT wavefunction

To calculate the $H_{\text{PNC}}^{\text{NSD}}$ induced electric dipole transition amplitude $E1_{\text{PNC}}^{\text{NSD}}$ with MBPT, we use the wavefunction in Eq. (16). For the purpose of using MBPT

calculations as the basics of analyzing the PRCC, it is sufficient to consider the total wave operator

$$\Omega = \Omega_{v,0}^{(1)} + \Omega_{v,1}^{(0)}. \quad (40)$$

The PNC induced $E1$ transition amplitude is then

$$E1_{\text{PNC}}^{\text{NSD}} = \langle \Phi_w \| \left[1 + \Omega_{w,0}^{(1)} + \lambda \Omega_{w,1}^{(0)} \right]^\dagger \mathbf{D} \left[1 + \Omega_{v,0}^{(1)} + \lambda \Omega_{v,1}^{(0)} \right] \| \Phi_v \rangle. \quad (41)$$

The expressions arising from these terms contain all the symmetry information to describe the properties of $T^{(1)}$. Consider terms linear in λ ,

$$E1_{\text{PNC}}^{\text{NSD}} = \langle \Phi_w \| \mathbf{D} \Omega_{v,1}^{(0)} + \Omega_{w,1}^{(0) \dagger} \mathbf{D} + \Omega_{v,0}^{(1) \dagger} \mathbf{D} \Omega_{v,1}^{(0)} + \Omega_{w,1}^{(0) \dagger} \mathbf{D} \Omega_{v,0}^{(1)} \| \Phi_v \rangle. \quad (42)$$

This is the MBPT expression of $E1_{\text{PNC}}^{\text{NSD}}$, which has one order each of $H_{\text{PNC}}^{\text{NSD}}$ and residual Coulomb interactions. The diagrams which arises from $\mathbf{D} \Omega_{v,1}^{(0)}$ and $\Omega_{w,0}^{(1) \dagger} \mathbf{D} \Omega_{v,1}^{(0)}$ are shown in Fig. 6. A similar set of diagrams, which arise from $\Omega_{w,1}^{(0) \dagger} \mathbf{D}$ and $\Omega_{w,1}^{(0) \dagger} \mathbf{D} \Omega_{v,0}^{(1)}$, are obtained from interchanging $H_{\text{PNC}}^{\text{NSD}}$ and \mathbf{D} vertices in the diagrams. Besides providing insights on the nature of perturbed

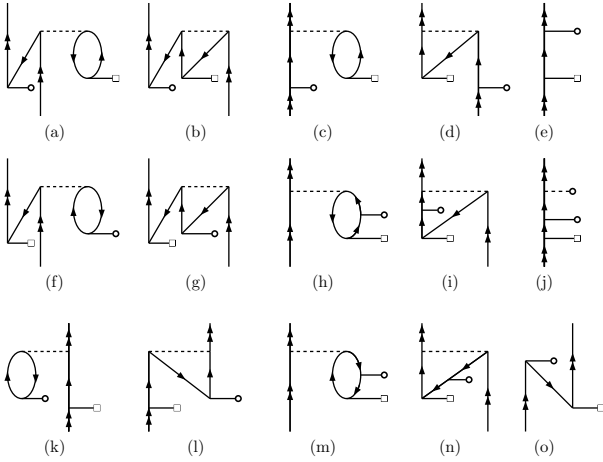


FIG. 6. $E1_{\text{elec}}^{\text{PNC}}$ diagrams which arise from the MBPT terms $\mathbf{D} \Omega_{v,1}^{(0)}$ and $\Omega_{w,0}^{(1) \dagger} \mathbf{D} \Omega_{v,1}^{(0)}$. These are the first and third terms of the Eq. (42). In the diagrams interaction lines terminated with circle and rectangle represent \mathbf{D} and $H_{\text{elec}}^{\text{PNC}}$, respectively.

cluster operators, detailed MBPT calculations serve another valuable purpose. These serve as reference calculations to validate the PRCC implementations.

B. From PRCC wavefunction

Like in MBPT, from the expression of the PRCC wave function in Eq. (33), the $H_{\text{PNC}}^{\text{NSD}}$ induced $E1$ transition

amplitude is

$$E1_{\text{PNC}}^{\text{NSD}} = \langle \Phi_w \| e^{T^\dagger} \left[1 + \lambda \mathbf{T}^{(1)} \cdot \mathbf{I} \right]^\dagger \left[1 + S + \lambda \mathbf{S}^{(1)} \cdot \mathbf{I} \right]^\dagger \mathbf{D} \times e^T \left[1 + \lambda \mathbf{T}^{(1)} \cdot \mathbf{I} \right] \left[1 + S + \lambda \mathbf{S}^{(1)} \cdot \mathbf{I} \right] \| \Phi_v \rangle. \quad (43)$$

Retain terms linear in λ as the remaining are zero from parity selection rule. Considering only the electronic component, like in the calculation of the cluster amplitudes $\mathbf{T}^{(1)}$ and $\mathbf{S}^{(1)}$, define $E1_{\text{elec}}^{\text{NSD}}$ as the $H_{\text{elec}}^{\text{NSD}}$ induced $E1$ amplitude in the electronic space. From the commutation relation of the cluster-operators, the expression is reduced to

$$E1_{\text{elec}}^{\text{NSD}} = \langle \Phi_w \| \bar{\mathbf{D}} \left[\mathbf{T}^{(1)} + \mathbf{S}^{(1)} + \mathbf{T}^{(1)} S \right] + \left[\mathbf{T}^{(1)} + \mathbf{S}^{(1)} + \mathbf{T}^{(1)} S \right]^\dagger \bar{\mathbf{D}} + S^\dagger \bar{\mathbf{D}} \left[\mathbf{T}^{(1)} + \mathbf{S}^{(1)} + \mathbf{T}^{(1)} S \right] + \left[\mathbf{T}^{(1)} + \mathbf{S}^{(1)} + \mathbf{T}^{(1)} S \right]^\dagger \bar{\mathbf{D}} S \| \Phi_v \rangle, \quad (44)$$

where $\bar{\mathbf{D}} = e^{T^\dagger} \mathbf{D} e^T$, is the dressed electric dipole operator. It is evident that $\bar{\mathbf{D}}$ is a non-terminating series of the closed-shell cluster operators. It is non-trivial to incorporate T to all orders in numerical computations. For this reason $\bar{\mathbf{D}}$ approximated as

$$\bar{\mathbf{D}} \approx \mathbf{D} + \mathbf{D} T^{(0)} + T^{(0) \dagger} \mathbf{D} + T^{(0) \dagger} \mathbf{D} T^{(0)}. \quad (45)$$

This captures all the important contributions arising from the core-polarization and pair-correlation effects. Terms not included in this approximation are terms which are third and higher order in $T^{(0)}$. The expression used in our calculations is then

$$E1_{\text{elec}}^{\text{NSD}} \approx \langle \Phi_w \| \mathbf{D} T^{(1)} + T^{(0) \dagger} \mathbf{D} T^{(1)} + \mathbf{T}^{(1) \dagger} \mathbf{D} T^{(0)} + \mathbf{T}^{(1) \dagger} \mathbf{D} + \mathbf{D} T^{(1)} S^{(0)} + \mathbf{T}^{(1) \dagger} S^{(0) \dagger} \mathbf{D} + S^{(0) \dagger} \mathbf{D} T^{(1)} + \mathbf{T}^{(1) \dagger} \mathbf{D} S^{(0)} + \mathbf{D} S^{(1)} + \mathbf{S}^{(1) \dagger} \mathbf{D} + S^{(0) \dagger} \mathbf{D} S^{(1)} + \mathbf{S}^{(1) \dagger} \mathbf{D} S^{(0)} \| \Phi_v \rangle. \quad (46)$$

The Eq. (46), as mentioned earlier, includes term up to second order in cluster amplitudes. From our previous study of properties calculations [25], we conclude that the contributions from the higher order are negligible. Selected diagrams from the leading-order and next to leading order terms of Eq. (46) are shown in the Fig. 7.

V. COUPLING WITH NUCLEAR SPIN

The PRCC diagrams of $E1_{\text{elec}}^{\text{NSD}}$ in Fig. 7 are, as explained earlier, defined in the electronic subspace. To calculate $E1_{\text{PNC}}^{\text{NSD}}$, the nuclear spin part of the operator is coupled with $E1_{\text{elec}}^{\text{NSD}}$. The $E1_{\text{PNC}}^{\text{NSD}}$ diagrams must then include a vertex which operates on the nuclear spin states. This is evident from the example MBPT diagram in Fig.

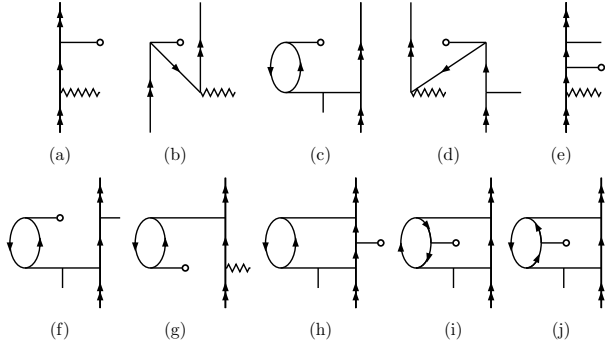


FIG. 7. Few of the leading order PRCC diagrams which contribute to the $E1_{\text{elec}}^{\text{PNC}}$ of one-valence atoms.

1(a). Although complicated, the coupling with the nuclear part of the operator require only angular integration, whereas the evaluation in the electronic space involves radial integrals. In our calculations, we use diagrammatic to carry out the angular integrals and as mentioned earlier, we follow the conventions of Lindgren and Morrison [28].

To elaborate on the coupling schemes, we discuss specific cases involving single and double PRCC operators. For the former, we select the topologically simplest, and for the later, one of the more complicated one. So that, these represent the range of topology and complexity of the diagrams. In each of these the main objective is to reduce the electronic part to a form common to a set of diagrams. And then, combine with the nuclear part.

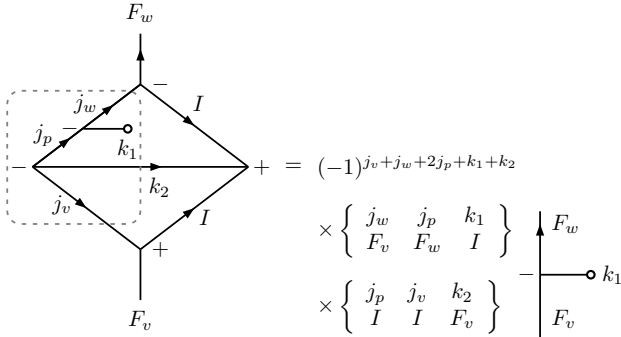


FIG. 8. Angular factor calculation of the $E1_{\text{PNC}}^{\text{NSD}}$ diagram shown in Fig. 7(a) and it arises from the term $DS_1^{(1)}$. The portion within the rectangle in dashed line indicate the electronic part. Remaining portion is from the nuclear spin and hyperfine coupling.

A. Singles PRCC operator

To define the coupling of singles diagrams, either $\mathbf{T}_1^{(1)}$ or $\mathbf{S}_1^{(1)}$, with nuclear spin part consider the diagram in

Fig. 7(a). It represents the Dirac-Fock contribution and is perhaps the simplest diagram. But it is the most dominant and naturally the most important. It is one of the diagrams arising from $DS_1^{(1)}$ in the PRCC calculations. The angular diagram for the electronic part of this diagram has same topology as in Fig. 7(a). However, the orbitals lines are replaced by angular momentum lines and arrows on appropriate lines to represent phase factors. The angular momentum diagram, which includes coupling with the nuclear spin, is shown in Fig. 8. The electronic part is the portion enclosed with the dashed line rectangle.

In the diagram, j_v and j_w are the total angular momentum of the single particle states of the initial and final one-valence atomic states, respectively. The line k_1 represents a rank one multipole line and denotes the angular part of the dipole operator. The multipole line k_2 is the all important representation of $H_{\text{PNC}}^{\text{NSD}}$, it is rank one multipole in electronic part as well as the nuclear part. In the electronic part, it represents the angular part of operator α and produces a transition from j_v to j_p . Here, j_p is the total angular momentum of the intermediate single particle state. On the other hand, in the nuclear sector, k_2 represents the operator \mathbf{I} . Since it is diagonal operator of the nuclear spin state $|I\rangle$, the k_2 line does not change the nuclear spin.

The last step in the angular momentum diagram representation is to couple the electron and nuclear momenta to form the total angular momentum of the hyperfine states. The initial and final hyperfine states are $|F_v\rangle$ and $|F_w\rangle$, respectively. The lines marked as F_v and F_w represent the angular momenta of the hyperfine states in the diagram. Using Wigner-Eckert theorem, we can write algebraic equivalent of the diagram as

$$\begin{aligned}
 \langle F_w m_w | DS_1^{(1)} \cdot \mathbf{I} | F_v m_v \rangle &= (-1)^{F_w - m_w} \begin{pmatrix} F_w & 1 & F_v \\ -m_w & q & m_v \end{pmatrix} \\
 &\times \langle F_w || D_{\text{eff}} || F_v \rangle, \quad (47)
 \end{aligned}$$

where $D_{\text{eff}} = DS_1^{(1)} \cdot \mathbf{I}$ is a rank one operator, m_i are the hyperfine magnetic quantum numbers and q is the component of D_{eff} . The phase factor and $3j$ -symbol in the above expression are the free lines in the right hand side of the diagrammatic equation in Fig. 8. Remaining expression on the right hand side, phase factor and $6j$ -symbols, is the m independent angular component of $\langle F_w || D_{\text{eff}} || F_v \rangle$.

B. Doubles PRCC operator

For the coupling with nuclear spin involving either $\mathbf{T}_1^{(1)}$ or $\mathbf{S}_1^{(1)}$, consider a more complicated diagram as shown in Fig. 9(a). It is the exchange of diagram in Fig. 7(j) and arises from the term $T_2^{(0)\dagger} DS_2^{(1)}$ in the PRCC expression of $E_{\text{elec}}^{\text{NSD}}$. The angular momentum diagram is shown in Fig. 9(b) and note that the angular momentum representation of $\mathbf{S}_2^{(1)}$ is as described in Section. III. The labels

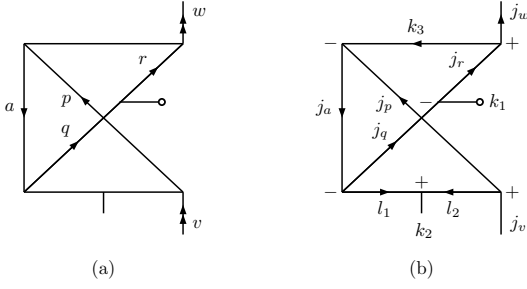


FIG. 9. Angular momentum diagram representation of a PRCC $E1_{\text{elec}}^{\text{NSD}}$ diagram. (a) Exchange of the diagram shown in Fig. 7(j). (b) The corresponding angular momentum diagram.

of the lines are different from the one in Fig. 2, however, these are dummy labels and same selection rules apply to l_1 and l_2 , and k_2 represents a rank one multipole line. It has the same role in the electronic sector as k_2 of the diagram in Fig. 8.

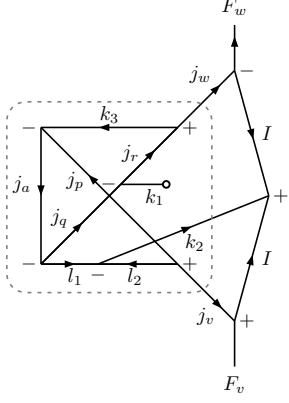


FIG. 10. Angular momentum diagram of $E1_{\text{PNC}}^{\text{NSD}}$ in the hyperfine states involving double excitation cluster operator $S_2^{(1)}$. The diagram arises from the term $S_2^{(0)\dagger} \mathbf{D} S_2^{(1)}$ and the portion within the rectangle in dashed lines indicate the portion arising from the electronic sector.

To demonstrate the non-trivial angular integration in the calculations with hyperfine atomic states, the angular momentum diagram of $\langle F_w m_w | T_2^{(0)\dagger} \mathbf{D} S_2^{(1)} \cdot \mathbf{I} | f_v m_v \rangle$, of the diagram in Fig. 9, is shown in Fig. 10. The portion of the diagram within the rectangle in dashed-line is the angular momentum part of the electronic sector and except for the topological rotation of the (l_1, l_2, k_2) vertex, it is identical to the diagram in Fig. 9(b). The evaluation of the angular integral of the electronic sector, for the example considered, is shown in Fig. 11. Important point to be observed is the structure of the free part in the right hand side of the diagrammatic equation in Fig. 11. Although the multipole lines of D and α , k_1 and k_2 respectively, are coupled to an effective multipole l_4 ,

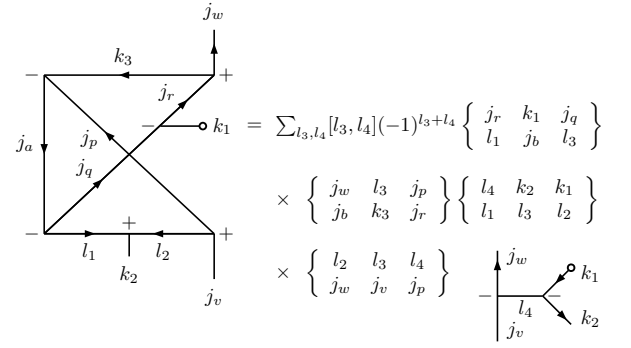


FIG. 11. Angular factor reduction in the electronic sector. The angular momentum diagram on the left hand side is the portion within rectangle in Fig. 10. On the right hand side, the angular momentum diagram with free lines represents the effective part coupled to the nuclear spin.

the k_1 and k_2 are present as free lines. The effective multipole l_4 operates on j_v and transforms it to j_w . In terms of Wigner-Eckert theorem, the diagram is equivalent to

$$\begin{aligned} &\langle j_w m_w | \sum_{l_4} \left\{ T_2^{(0)\dagger} \mathbf{D} S_1^{(1)} \right\}^{l_4} | j_v m_v \rangle = (-1)^{j_w - m_w} \\ &\times \left(\begin{matrix} j_w & l_4 & j_v \\ -m_w & q & m_v \end{matrix} \right) \langle j_w || \left\{ T_2^{(0)\dagger} \mathbf{D} S_1^{(1)} \right\}^{l_4} || j_v \rangle, \quad (48) \end{aligned}$$

where $\{\dots\}^{l_4}$ represents coupling of rank one tensor operators \mathbf{D} and $\mathbf{S}^{(1)}$ to an operator of rank l_4 . This coupling is a structure common to any PRCC term of $E1_{\text{elec}}^{\text{NSD}}$. That is, for any term, the angular integral in the electronic sector is reducible to a form where the free lines is similar to the one on the right hand side of Fig. 11. From the triangular condition, $l_4 = 0, 1, 2$ are the al-

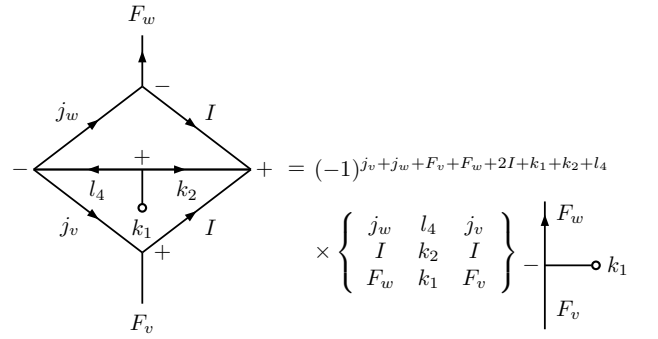


FIG. 12. Angular factor reduction of the coupling between the electronic sector with the nuclear spin of a diagram arising from $S_2^{(0)\dagger} \mathbf{D} S_2^{(1)}$. The electronic sector of the diagram is shown in Fig. 11.

lowed values, however, what values of l_4 contribute depends on j_v and j_w . For example, $l_4 = 0, 1$ contribute in the PNC $6^2S_{1/2} \rightarrow 7^2S_{1/2}$ transition of atomic Cs [2],

where as only $l_4 = 2$ contributes to the proposed PNC $6\ ^2S_{1/2} \rightarrow 5\ ^2D_{5/2}$ transition in Ba^+ [3].

The form of the free lines in the Fig. 11 require one due consideration while combining with the nuclear part. It is the multipole line k_2 , inherited from $\mathbf{T}^{(1)}$ or $\mathbf{S}^{(1)}$, which couples with the operator \mathbf{I} to form a scalar operator. The diagrammatic representation is shown on the left side of Fig. 12. After evaluation, it reduces to a $9j$ -symbol and free line part. From Wigner-Eckert theorem, the matrix element in the hyperfine states is

$$\sum_{l_4} \langle F_w m_w | \left\{ \left[T_2^{(0)\dagger} \mathbf{D} \mathbf{S}_1^{(1)} \right]^{l_4} \mathbf{I} \right\}^1 | F_v m_v \rangle = (-1)^{F_w - m_w} \times \begin{pmatrix} F_w & 1 & F_v \\ -m_w & q & m_v \end{pmatrix} \langle F_w \| D_{\text{eff}} \| F_v \rangle, \quad (49)$$

where

$$D_{\text{eff}} = \left\{ \left[T_2^{(0)\dagger} \mathbf{D} \mathbf{S}_1^{(1)} \right]^{l_4} \mathbf{I} \right\}^1, \quad (50)$$

is the effective dipole operator in the hyperfine states. It is of the same form as the effective operator in Eq. (47). However, the coupling sequence in Eq. (49) is general and applies to all the terms in the $E1_{\text{PNC}}^{\text{NSD}}$.

VI. VALIDATION OF PRCC

The RCC method described so far involves intricate but tractable angular momentum coupling and most of the calculations are in the configuration space of reduced dimension, namely of the electrons. Considering the complexity of the method, it is desirable to validate the method with few selected terms before a full scale implementation. Here, we present a method of validation by comparing with dominant third order MBPT diagrams. This is possible as we solve the PRCC equations iteratively with the first order MBPT wave functions as the initial guess. In particular, we evaluate the $E1_{\text{PNC}}^{\text{NSD}}$ of the transition $6s \rightarrow 7s$ in ^{133}Cs .

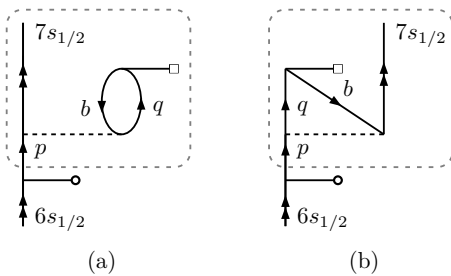


FIG. 13. MBPT $E1_{\text{PNC}}^{\text{NSD}}$ diagrams used in the validation of the the singles PRCC amplitudes $S_1^{(1)}$.

TABLE I. Validation of singles PRCC amplitudes. The values listed are in units of $iea_0\mu'_w$. Numbers in the square bracket represent the power of 10.

Orbital (p, q)	MBPT	PRCC
$6p_{1/2}$	3.80237[-15]	3.80237[-15]
$7p_{1/2}$	-4.42335[-16]	-4.42335[-16]
$8p_{1/2}$	1.08456[-16]	1.08456[-16]
$9p_{1/2}$	1.88997[-16]	1.88997[-16]
$10p_{1/2}$	8.66134[-17]	8.66134[-17]
$11p_{1/2}$	2.41491[-18]	2.41491[-18]

A. Single excitation operator $S_1^{(1)}$

To check the PRCC equation and angular momentum coupling in the calculations of $S_1^{(1)}$, consider the term $S_1^{(1)\dagger} D$ in $E_{\text{PNC}}^{\text{NSD}}$. Two of the third order MBPT diagrams, which are equivalent to the $S_1^{(1)\dagger} D$ at the first iteration of the PRCC equation are shown in Fig. 13. In the figure, the portion of the diagrams within the rectangle of dashed-line arises from the second order wave operator $\Omega_{7s,1}^{(1)\dagger}$ define in Eq. (17). As for the solutions of linearized PRCC equations, the initial guess is the first order MBPT wave function $\Omega_{7s,1}^{(0)}$. Single excitation cluster amplitudes τ are then calculated iteratively from Eq. (30). At the first iteration of the linearized PRCC equation, the diagram within the dashed rectangle in Fig. 13(a) is equal to the one valence version of the diagram in Fig. 4(c). And, the diagram Fig. 13(b) is the exchange counterpart. These MBPT diagrams are the dominant ones after the DF and other theories like the PRCC must be able to reproduce matching results.

For comparison, $E1_{\text{PNC}}^{\text{NSD}}$ contribution from the two diagrams in Fig. 4 from MBPT and results from the equivalent PRCC calculations are listed in Table. I. The specific orbital wise contributions, for better comparison, of the dominant contributions are listed in the table. It is evident that there is excellent agreement between the MBPT and PRCC results.

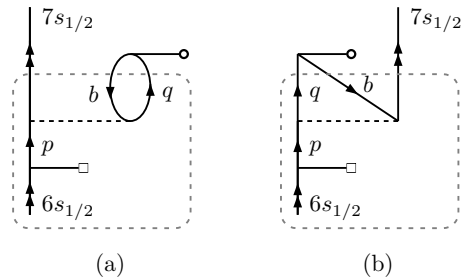


FIG. 14. MBPT $E1_{\text{PNC}}^{\text{NSD}}$ diagrams used in the validation of the doubles PRCC amplitudes $S_2^{(1)}$.

B. Double excitation operator $S_2^{(1)}$

Like in the case of $S_1^{(1)}$, consider two MBPT diagrams which are equivalent to the $S_2^{(1)}$ diagram after the first iteration and are shown in Fig. 14. In the figure, the portion of the diagrams within the rectangle in dashed-lines are equivalent to the $S_2^{(1)}$ diagram in Fig. 5(a) but adapted for one-valence systems. However, there is a major difference from the $S_1^{(1)}$. As $H_{\text{PNC}}^{\text{NSD}}$ is a single particle operator, the double excitation cluster operator at one order of $H_{\text{PNC}}^{\text{NSD}}$ is zero and the initial guess value is set to zero. To provide a wider test sample, for the double excitation the MBPT diagrams considered are equivalent to the term $DS_2^{(1)}$ in PRCC. Another variation is, the two diagrams considered in $S_1^{(1)}$ arise from topologically different diagrams, in the present case, the two diagrams in Fig. 14 arise from the same $S_2^{(1)}$ but different cluster amplitudes.

TABLE II. Validation of doubles PRCC amplitudes. The values listed are in units of $iea_0\mu'_w$. Numbers in the square bracket represent the power of 10.

Orbital (p, q)	MBPT	PRCC
$6p_{1/2}$	6.53322[-17]	6.53322[-17]
$7p_{1/2}$	2.35102[-17]	2.35102[-17]
$8p_{1/2}$	3.20651[-16]	3.20651[-16]
$9p_{1/2}$	2.02539[-15]	2.02539[-15]
$10p_{1/2}$	8.67435[-16]	8.67435[-16]
$11p_{1/2}$	3.02443[-17]	3.02443[-17]

The results from the MBPT and PRCC calculations are listed in Table. II. Here too, the results from the two calculations are in excellent agreement. Perhaps, it must be mentioned that, the angular momentum factor calculations of the MBPT and PRCC diagrams are done in very different steps. Electronic part of the portion within the rectangle in dashed-line in Fig. 14 are evaluated to reduce to the representation of $S_2^{(1)}$ as discussed in Section. IIIB. MBPT diagrams, on the other hand, may be evaluated without the need to associate with an effective operator of specific form.

VII. CONCLUSIONS

The relativistic coupled-cluster method we have developed to incorporate a nuclear spin-dependent perturbation is an apt one to calculate nuclear spin-dependent parity non-conservation in atoms and ions. The representation of the cluster amplitude within the electronic sector as a tensor operator of rank one and coupling with the nuclear spin part at a later stage of property calculation leads to simplification of the calculations. Otherwise, the entire calculation must be done with hyperfine states, which involves complicated angular momen-

tum couplings at all stages of the calculations. The proposed scheme, on the other hand, introduces the nuclear spin coupling is with a simplified effective operator in the electronic sector. The validity of the representation is explicitly tested and verified with selected diagrams. Although limited in number, the diagrams and terms selected in the sample test calculations are varied enough to account for complex as well as subtle issues related to the method. Based on the results presented, we conclude that the method works and in future publications we shall report results of sophisticated and large scale calculations using PRCC.

ACKNOWLEDGMENTS

We wish to thank S. Chattopadhyay, S. Gautam, K. V. P. Latha, B. Sahoo and S. A. Silotri for useful discussions. The results presented in the paper are based on computations using the HPC cluster at Physical Research Laboratory, Ahmedabad.

Appendix: Angular factors of PRCC equation

Here, we give the linearized PRCC equations of the closed-shell sector, Eqs. (30) and (31), after angular integration. The one-valence cluster amplitude equations can be obtained after suitable modifications.

1. Single excitation cluster operator

The angular reduction of each diagram is such that the free parts are reduced to the form in Fig. 3(a). The free part is common to all the diagrams and is avoided in the computational implementation. So, solutions of the PRCC equations are the cluster amplitudes in reduced matrix form. For $T_1^{(1)}$ and $S_1^{(1)}$, the rank of the operator, and hence the free part, is one. For convenience, the representation of $T_2^{(1)}$ is redefined as

$$\mathbf{T}_2^{(1)} = \sum_{abpq} \sum_{l_1, l_2} \tau_{ab}^{pq}(l_1, l_2) \{ \mathbf{C}_{l_1}(\hat{r}_1) \mathbf{C}_{l_2}(\hat{r}_2) \}^1. \quad (\text{A.1})$$

Like the PRCC operators, we use t_a^p and t_{ab}^{pq} to represent the unperturbed single and double excitation amplitudes, respectively. The tensor operator structure of $T_2^{(0)}$ is

$$T_2^{(0)} = \sum_{abpq} \sum_k t_{ab}^{pq}(k) \mathbf{C}_k(\hat{r}_1) \cdot \mathbf{C}_k(\hat{r}_2). \quad (\text{A.2})$$

For the Slater integrals, the reduced matrix element is

$$X_k(abcd) = (-1)^k \langle \kappa_a \| \mathbf{C}^k \| \kappa_c \rangle \langle \kappa_b \| \mathbf{C}^k \| \kappa_d \rangle R_k(abcd), \quad (\text{A.3})$$

where, $R_k(abcd)$ is the radial part of the Slater integral. With these definitions, the Eq. (30) is written in terms of reduced matrix elements and appropriate angular factors.

$$\begin{aligned}
(\epsilon_a - \epsilon_p)\tau_a^p &= \mathbf{h}_{pa} + \sum_q \frac{\delta(j_a, j_q)}{\sqrt{(2j_a + 1)}} \mathbf{h}_{pq} t_a^q - \sum_b \frac{\delta(j_b, j_p)}{\sqrt{(2j_b + 1)}} \mathbf{h}_{ba} t_b^p + \sum_{bqk_2} \mathbf{h}_{bq} \left[\frac{\delta(k_1, k_2)}{\sqrt{(2k_1 + 1)}} (-1)^{j_q - j_b + k_1} t_{ba}^{qp}(k_2) \right. \\
&\quad \left. - (-1)^{j_b + j_q + k_1} \begin{Bmatrix} j_b & j_q & k_1 \\ j_a & j_p & k_2 \end{Bmatrix} t_{ab}^{qp}(k_2) \right] + \sum_{bqk_2} \tau_b^q \left[\frac{\delta(k_1, k_2)}{\sqrt{(2k_1 + 1)}} (-1)^{j_q - j_b + k_1} X_{k_2}(bpqa) \right. \\
&\quad \left. - (-1)^{j_b + j_q + k_1} \begin{Bmatrix} j_a & j_b & k_2 \\ j_q & j_p & k_1 \end{Bmatrix} X_{k_2}(bpaq) \right] + \sum_{bqrk_2} \sum_{l_1 l_2} \tau_{ba}^{qr}(l_1, l_2) \left[\frac{\delta(k_2, l_2)}{\sqrt{(2k_2 + 1)}} (-1)^{j_q - j_b + j_a + j_p + l_1} \right. \\
&\quad \times \left. \begin{Bmatrix} j_r & j_a & l_1 \\ k_1 & k_2 & j_p \end{Bmatrix} X_{k_2}(bpqr) - (-1)^{j_a + j_p + j_b + j_q + l_1} \begin{Bmatrix} j_b & k_2 & j_r \\ j_p & l_2 & j_q \end{Bmatrix} \begin{Bmatrix} j_r & j_a & l_1 \\ k_1 & l_2 & j_p \end{Bmatrix} X_{k_2}(bprq) \right] \\
&\quad - \sum_{bcqk_2} \sum_{l_1 l_2} X_{k_2}(bcqa) \left[\frac{\delta(k_2, l_2)}{\sqrt{(2k_2 + 1)}} (-1)^{j_a - j_b + j_p + j_q + k_1 + k_2} \begin{Bmatrix} j_p & l_1 & j_c \\ k_2 & j_a & k_1 \end{Bmatrix} \tau_{bc}^{qp}(l_1, l_2) \right. \\
&\quad \left. - (-1)^{j_q + j_c + j_a + j_p + k_1 + l_2} \begin{Bmatrix} k_2 & j_a & j_c \\ l_2 & j_q & j_b \end{Bmatrix} \begin{Bmatrix} j_b & j_p & l_1 \\ k_1 & l_2 & j_a \end{Bmatrix} \tau_{cb}^{qp}(l_1, l_2) \right]. \tag{A.4}
\end{aligned}$$

2. Double excitation cluster operator

For the double excitation PRCC operator $T_2^{(1)}$, the common free part of the angular factors in Eq. (31) is

as shown in Fig. 3(b). In the angular factors, the multipoles k_1 , k_2 , l_1 and l_2 have the same interpretations as in the singles. Multipoles l_3 and l_4 are, however, arise from coupling (j_a, j_p) and (j_b, j_q) , respectively. The double excitation cluster equation obtained from the projection on $\langle \Phi_{ab}^{pq} |$ along with appropriate angular factors is

$$\begin{aligned}
(\epsilon_a + \epsilon_b - \epsilon_p - \epsilon_q)\tau_{ab}^{pq}(l_1, l_2) &= \left[\sum_r (2l_1 + 1) (-1)^{j_a + j_p + k_1 + l_2} \begin{Bmatrix} k_1 & j_p & j_r \\ j_a & l_2 & l_1 \end{Bmatrix} \mathbf{h}_{pr} t_{ab}^{rq}(l_2) - \sum_c (2l_1 + 1) \right. \\
&\quad \times (-1)^{j_a + j_p + l_1} \begin{Bmatrix} k_1 & j_a & j_c \\ j_p & l_2 & l_1 \end{Bmatrix} \mathbf{h}_{ca} t_{cb}^{pq}(l_2) + \sum_r (2l_1 + 1) (-1)^{j_a + j_p + l_1} \begin{Bmatrix} l_2 & j_p & j_r \\ j_a & k_1 & l_1 \end{Bmatrix} X_{l_2}(pqr b) \tau_a^r \\
&\quad - \sum_c (2l_1 + 1) (-1)^{j_a + j_p + k_1 + l_2} \begin{Bmatrix} l_2 & j_a & j_c \\ j_p & k_1 & l_1 \end{Bmatrix} X_{l_2}(cqab) \tau_c^p + \sum_{rc} \frac{1}{(2l_1 + 1)} (-1)^{j_r - j_c + l_1} \\
&\quad \times X_{k_2}(pcar) \tau_{cb}^{rq}(l_1, l_2) - \sum_{rc} \sum_{l_3 l_4} (2l_2 + 1) (-1)^{j_c - j_q + k_1 + l_3} \begin{Bmatrix} j_r & l_3 & j_b \\ j_c & l_4 & j_q \\ l_1 & k_1 & l_2 \end{Bmatrix} X_{l_1}(pcar) \tau_{bc}^{rq}(l_3, l_4) \\
&\quad - \sum_{rck_2} \sum_{l_3 l_4} (2l_1 + 1) (2l_2 + 1) (-1)^{j_a + j_p + j_b + j_q + k_1} \begin{Bmatrix} k_2 & j_p & j_r \\ j_a & l_3 & l_1 \end{Bmatrix} \begin{Bmatrix} l_2 & l_1 & k_1 \\ l_3 & l_4 & k_2 \end{Bmatrix} \begin{Bmatrix} k_2 & j_c & j_b \\ j_q & l_2 & l_4 \end{Bmatrix} X_{k_2}(pcrb) \\
&\quad \times \tau_{ac}^{rq}(l_3, l_4) - \sum_{rck_2} (-1)^{j_c + j_r + l_3} \begin{Bmatrix} j_a & j_c & k_2 \\ j_r & j_p & l_1 \end{Bmatrix} X_{k_2}(cpar) \tau_{cb}^{rq}(l_1, l_2), \left. \right] + \left[\begin{array}{l} p \leftrightarrow q \\ a \leftrightarrow b \end{array} \right] \\
&\quad + \sum_{rsk_2} \sum_{l_3 l_4} (2l_1 + 1) (2l_2 + 1) (-1)^{j_a + j_p + j_b + j_q + k_1 + k_2 + l_4 + l_2} \begin{Bmatrix} k_2 & j_p & j_r \\ j_a & l_3 & l_1 \end{Bmatrix} \begin{Bmatrix} l_1 & l_3 & k_2 \\ l_4 & l_2 & k_1 \end{Bmatrix} \begin{Bmatrix} k_2 & j_s & j_q \\ j_b & l_2 & l_4 \end{Bmatrix} \\
&\quad \times X_{k_2}(pqrs) \tau_{ab}^{rs}(l_3, l_4) + \sum_{cdk_2} \sum_{l_3 l_4} (2l_1 + 1) (2l_2 + 1) (-1)^{j_a + j_p + j_b + j_q + k_1 + k_2 + l_3 + l_1} \begin{Bmatrix} k_2 & j_a & j_c \\ j_p & l_3 & l_1 \end{Bmatrix} \\
&\quad \times \begin{Bmatrix} l_2 & l_1 & k_1 \\ l_3 & l_4 & k_2 \end{Bmatrix} \begin{Bmatrix} k_2 & j_d & j_b \\ j_q & l_2 & l_4 \end{Bmatrix} X_{k_2}(cdab) \tau_{cd}^{pq}(l_3, l_4). \tag{A.5}
\end{aligned}$$

-
- [1] Y. Zel'dovich, JETP **6**, 1184 (1958).
- [2] C. S. Wood, et al. Science **275**, 1759 (1997).
- [3] N. Fortson, Phys. Rev. Lett. **70**, 2383 (1993).
- [4] K. Tsigutkin, D. Dounas-Frazer, A. Family, J. E. Stalnaker, V. V. Yashchuk, and D. Budker, Phys. Rev. Lett. **103**, 071601 (2009); Phys. Rev. A **81**, 032114 (2010).
- [5] B. K. Sahoo, P. Mandal and M. Mukherjee, Phys. Rev. A **83**, 030502 (2011).
- [6] V. A. Dzuba and V. V. Flambaum, Phys. Rev. A **83**, 042514 (2011).
- [7] V. A. Dzuba, V. V. Flambaum, and M. G. Kozlov, Phys. Rev. A **54**, 3948 (1996).
- [8] S. G. Porsev, M. G. Kozlov, and Yu. G. Rakhlin, Hyperfine Interact. **127**, 395 (2000).
- [9] V. A. Dzuba, V. V. Flambaum, arXiv:1104.0086.
- [10] K. P. Geetha, A. D. Singh, B. P. Das, and C. S. Unnikrishnan, Phys. Rev. A **58**, R16 (1998).
- [11] A. D. Singh and B. P. Das, J. Phys. B **32**, 4905 (1999).
- [12] B. K. Mani and D. Angom, arXiv:1104.3473v1.
- [13] F. Coester, Nucl. Phys. **7**, 421 (1958).
- [14] F. Coester and H. Kümmel, Nucl. Phys. **17**, 477 (1960).
- [15] R. Pal, M. S. Safronova, W. R. Johnson, A. Derevianko, and S. G. Porsev, Phys. Rev. A **75**, 042515 (2007).
- [16] B. K. Sahoo, L. W. Wansbeek, K. Jungmann, and R. G. E. Timmermans, Phys. Rev. A **79**, 052512 (2009).
- [17] H. S. Nataraj, B. K. Sahoo, B. P. Das, and D. Mukherjee, Phys. Rev. Lett. **101**, 033002 (2008).
- [18] K. V. P. Latha, D. Angom, B. P. Das, and D. Mukherjee, Phys. Rev. Lett. **103**, 083001 (2009).
- [19] C. Thierfelder and P. Schwerdtfeger, Phys. Rev. A **79**, 032512 (2009).
- [20] B. K. Sahoo, B. P. Das, and D. Mukherjee, Phys. Rev. A **79**, 052511 (2009).
- [21] L. W. Wansbeek, B. K. Sahoo, R. G. E. Timmermans, K. Jungmann, B. P. Das, and D. Mukherjee, Phys. Rev. A **78**, 050501(R) (2008).
- [22] R. Pal, D. Jiang, M. S. Safronova, and U. I. Safronova, Phys. Rev. A **79**, 062505 (2009).
- [23] S. G. Porsev, K. Beloy, and A. Derevianko, Phys. Rev. D **82**, 036008 (2010).
- [24] B. K. Mani, K. V. P. Latha, and D. Angom, Phys. Rev. A **80**, 062505 (2009).
- [25] B. K. Mani and D. Angom, Phys. Rev. A **81**, 042514 (2010).
- [26] B. K. Sahoo and B. P. Das, Phys. Rev. A **77**, 062516 (2008).
- [27] K. V. P. Latha, D. Angom, R. K. Chaudhari, B. P. Das and D. Mukherjee, J. Phys. B. **41**, 035005 (2008).
- [28] I. Lindgren and J. Morrison, *Atomic Many-Body Theory*, edited by G. Ecker, P. Lambropoulos, and H. Walther (Springer-Verlag, 1985).
- [29] S. A. Blundell, W. R. Johnson, Z. W. Liu and J. Sapirstein, Phys. Rev. A **39**, 3768 (1989).
- [30] S. A. Blundell, W. R. Johnson, Z. W. Liu and J. Sapirstein, Phys. Rev. A **40**, 2233 (1989).
- [31] B. K. Mani and D. Angom, Phys. Rev. A **83**, 012501 (2011).